Progress In Electromagnetics Research Letters, Vol. 26, 39–48, 2011

PRINTED BLUETOOTH AND UWB ANTENNA WITH DUAL BAND-NOTCHED FUNCTIONS

F.-C. Ren*, **F.-S. Zhang, J.-H. Bao, Y.-C. Jiao, and L. Zhou**

National Laboratory of Antennas and Microwave Technology, Xidian University, Xi'an, Shaanxi 710071, China

Abstract—A novel hybrid design of Bluetooth and UWB antenna with dual band-notched functions is proposed. The proposed antenna structure consists of a microstrip-fed main patch and electromagnetically coupled parasitic patch with arc-shaped strips, achieving Bluetooth and UWB performance. Additionally, the split ring resonator (SRR) slot etched on the main patch and the square patch close to microstrip feedline are aimed to obtain dual notched bands. The numerical and experimental results exhibit that the designed antenna operates over the wide frequency band from 3 to more than 12 GHz, while showing the extra resonant mode at 2.4-GHz Bluetooth and the band rejection performance at 3.5-GHz WiMAX and 5.2-GHz WLAN.

1. INTRODUCTION

Ultrawideband (UWB) technology has gained a lot of popularity in wireless industry, which is marketed within the frequency band of 3.1 GHz to 10.6 GHz, released by the FCC in 2002 [1]. The attractiveness of UWB is its capability of offering high capacity short-range wireless links using low-energy transceivers. Planar monopole antennas have been found as good candidates for UWB applications owing to their attractive advantages, such as wide impedance bandwidth, ease of fabrication, and acceptable radiation properties. Recently, many types of monopole antennas on a curvilinear shape, such as circular, ellipse and annular ring, etc. [2–4], have been proposed for UWB applications. In addition, the hybrid antenna composed of a simple monopole and parasitic element is reported in [5]. The parasitic patch improves the impedance bandwidth for broadband operation

---

Received 3 July 2011, Accepted 15 August 2011, Scheduled 19 August 2011

* Corresponding author: Feng-Chao Ren (fchren@163.com).

in [6, 7]. Furthermore, the hybrid antenna is proposed for UWB application in [8]. Meanwhile, the combination of high-quality UWB technology, Bluetooth, operating at 2.4 GHz to 2.484 GHz, has been widely equipped in portable devices. Thus, the integrated Bluetooth and UWB antenna is proposed in [9]. On the other hand, the UWB band will cause interference to the existing wireless communication systems, for example wireless local area network (WLAN) operating in 5.15–5.35 GHz and worldwide interoperability for microwave access (WiMAX) system covering 3.4–3.69 GHz. Therefore, the UWB antenna with band-filtered performance is required to remove electromagnetic interference. Various methods, mainly divided into three categories, have been proposed for band-notched designs. The first category is carving slots on the radiation element, such as U-shaped, L-shaped, and T-shaped, etc. [10–12]. The second one is putting parasitic elements close to the radiator [13, 14]. Another way to realize band rejection is prefiltering signals by applying a filter structure into feedline [15, 16], which is independent and not affect the radiation property of antenna structure. Taken together what is said from above, a novel technique for simultaneously adding extra resonant mode and notched bands to UWB antenna is essential to fulfill all the standards.

In this paper, a novel parasitic-coupled monopole antenna is presented for Bluetooth and UWB applications. In the design, the main patch is directly fed by microstrip line, and the parasitic patch with arc-shaped strips along the top side is indirectly coupled to the main patch. The design skills are introduced to approach excitation of dual resonant modes for Bluetooth and UWB. Additionally, the SRR slot etched on main patch and the square patch close to feedline are aimed to obtain notched bands. The numerical and experimental results are discussed as follows.

2. ANTENNA DESIGN

Figure 1 shows the geometry of the proposed Bluetooth and UWB antenna with dual notched bands, which is printed on FR4 substrate with relative dielectric constant of 4.6 and thickness of 1.6 mm. In the antenna structure, the main patch in ellipse of half major axis a_1 and minor axis b_1, can provide the basic resonant frequency, and the parasitic patch in modified ellipse is used as parasitic resonator on the back surface of the substrate, electrically coupled to the main patch. The coupling between two patches reinforces the electric field density in the substrate, called it capacitive loading. As a result, the electrical length of the antenna is increased and the lower band-edge frequency

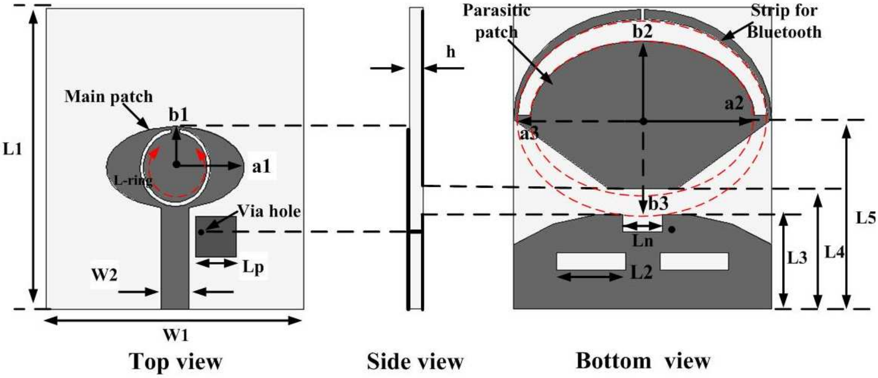

Figure 1. Geometry of the proposed antenna with notched bands.

decreases. Moreover, a pair of arc-shaped strips is attached along the top side of the parasitic patch for the purpose of extra resonant mode at 2.4-GHz Bluetooth.

In the band-notched antenna design, a split ring resonator (SRR) slot is etched on the main patch to implement rejected band at 3.5 GHz-WiMAX. The notched frequency f_{notch} can be empirically approximated by

$$f_{notch} = \frac{c}{\sqrt{\varepsilon_{eff}} \cdot \lambda_g} \approx \frac{c}{\sqrt{\varepsilon_{eff}} \cdot 2 \cdot l_{-ring}} \tag{1}$$

$$\varepsilon_{eff} \approx \frac{\varepsilon_r + 1}{2} \tag{2}$$

where c and ε_{eff} are the speed of light and the approximated effective dielectric constant, respectively; l_{-ring} is the total length of the split ring slot. Note that as the notched frequency increases, slot's length will decrease which results in a weaker notch, because the slot is very far from the edge of the patch on which the current mainly distributes. Therefore, the split ring slot is applied to resonate at 3.5 GHz, instead of 5.2 GHz. On the other hand, the square patch, placing close to microstrip feedline, is connected to the ground plane via metallic hole. The structure formed by a via-loaded metal patch can be characterized by a resonator, having the advantage of small volume and simple structure to obtain band-notched performance at 5.2 GHz-WLAN.

Regarding the rectangular slots carved on the ground plane, the structure provides an additional current path and changes the inductance or capacitance of the input impedance. Thus, much better impedance matching may be achieved in the antenna design.

3. RESULTS AND DISCUSSIONS

An electromagnetic software package, Ansoft HFSS, is utilized to analyze electrical features of the proposed antenna. By fine-tuning, the final optimal dimension values are obtained and listed in Table 1. As a practical example, a prototype was fabricated for validating feasibility of the proposed design. Figure 2 presents the photograph of fabricated antenna, and a 50 Ω-SMA connector is used to feed the antenna.

The simulated and measured reflection coefficients (S_{11}) of the proposed Bluetooth and UWB antenna are illustrated in Figure 3. Reasonable agreements between them are attained. Some slight discrepancies may be attributed to measurement errors, inaccuracies in the fabrication process, and the impact of the SMA connector. As observed, the antenna achieves good impedance matching from 3 to more than 12 GHz, while showing the extra resonant point at 2.4 GHz and band rejection performance around 3.5/5.2 GHz.

In order to explain the function of the parasitic element, different antennas with and without parasitic patch or strips are analyzed. Figure 4 shows the S_{11} variations of the different antenna versions, it is seen that the modified parasitic patch make the lower band-edge frequency decrease from 3.9 GHz to 3 GHz. Meanwhile, the arc-shaped

Table 1. The optimal antenna parameters (Unit: mm).

W_1	W_2	a_1	b_1	a_2	b_2	a_3	b_3
30	3.2	8	4.8	13	9.1	14.5	11.6
L_1	L_2	L_3	L_4	L_5	L_p	L_{-ring}	L_n
35	8	11	14	22	4.8	25.2	4.6


(a) (b)

Figure 2. Photograph of the fabricated prototype. (a) Top view. (b) Bottom view.

strips attached along the parasitic patch provide another resonant mode at 2.4 GHz. In the band-notched antenna design, the SRR slot is etched on the main patch, and the square patch laying aside the feedline is connected to the ground. However, a spurious notched band emerged in vicinity of undesired frequency of 8 GHz simultaneously, as shown in Figure 5. Interestingly, the spurious resonance is eliminated by etching rectangle slots to the ground plane, which changes current

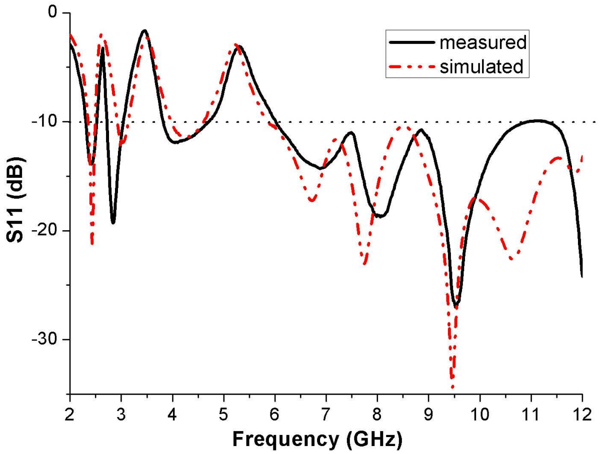

Figure 3. Simulated and measured S_{11} variations of the proposed antenna.

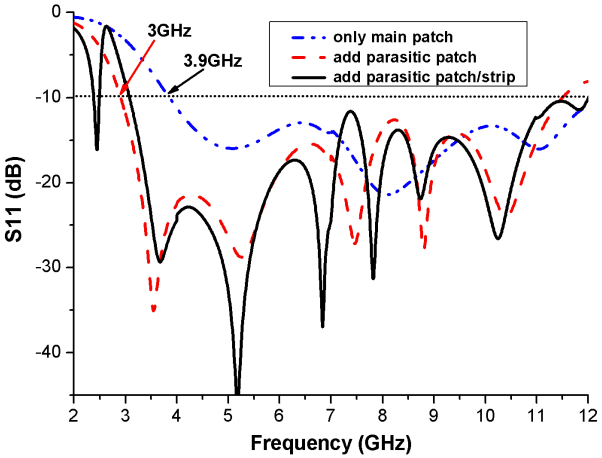

Figure 4. S_{11} variations of the different full-band antennas.

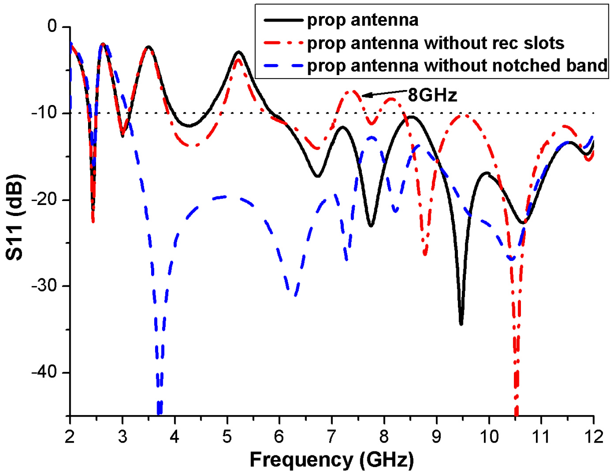

Figure 5. S_{11} variations of the different antennas with/without rectangle slots.

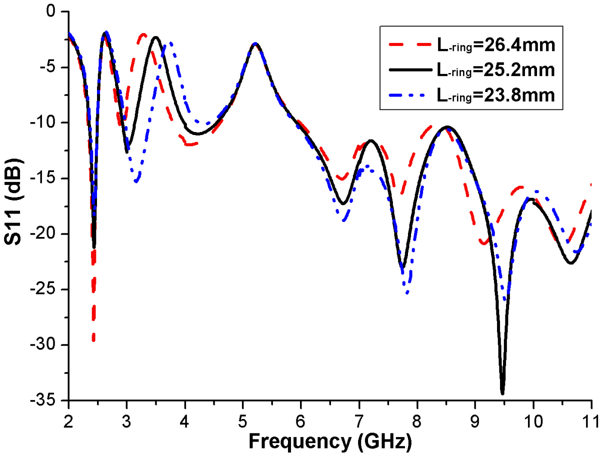

Figure 6. S_{11} variations for different values of SRR slot's length.

path and has better performance for impedance matching.

Now, the key parameters are analyzed for further investigation on notched bands. Simulated S_{11} curves for different values of l_{-ring} are illustrated in Figure 6, it is seen from the figure that the changing of the length of SRR slot has great impact on lower notch frequency with little effect on upper one. Figure 7 shows the effect of the various square patch width L_p on the S_{11} curves, suggesting that the upper

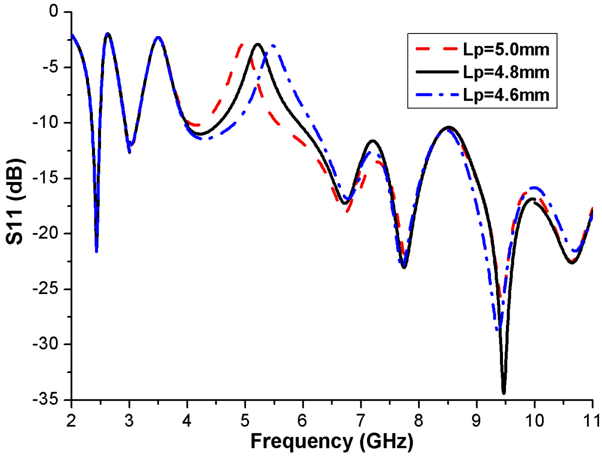

Figure 7. S_{11} variations for different values of square patch's width.

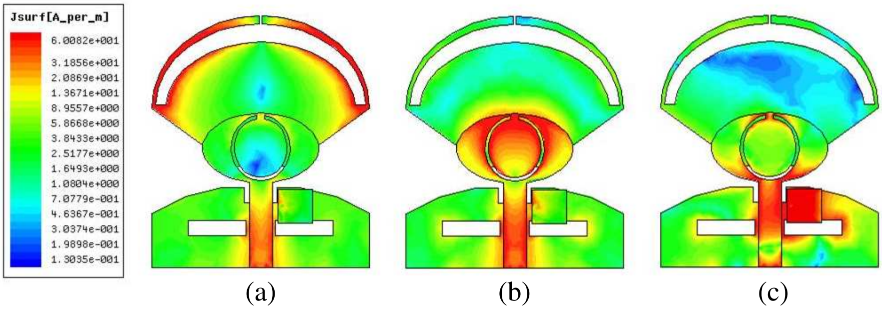

(a) (b) (c)

Figure 8. Surface current distribution at different frequencies. (a) 2.4 GHz. (b) 3.5 GHz. (c) 5.2 GHz.

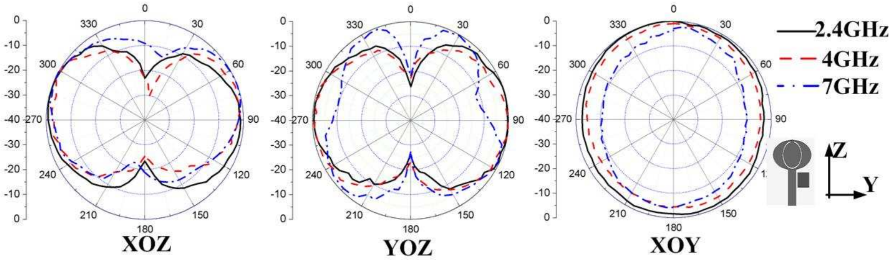

Figure 9. Radiation patterns in main cut planes.

rejected frequency can be tuned by adjusting the width of the patch.

For better understanding the behavior of the proposed antenna, surface current distributions at 2.4, 3.5, and 5.2 GHz are displayed in Figure 8. It is seen that the current distribution around strips along the parasitic patch is drastically increased at 2.4 GHz. Meanwhile, the obviously increased current distributions around SRR slot and square patch occur at 3.5 and 5.2 GHz, indicating that the SRR slot and square

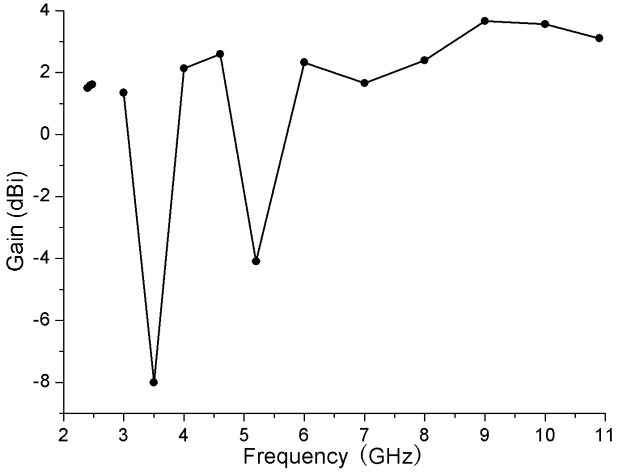

Figure 10. Variations of the realized gain with frequency.

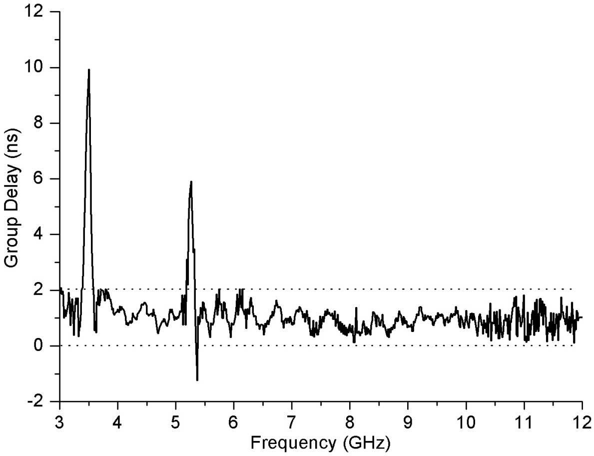

Figure 11. Group delay of the proposed antenna transfer system.

patch introduce the band-rejected function at the relevant frequency.

The radiation patterns in main cut planes at 2.4 GHz, 4 GHz and 7 GHz are shown in Figure 9. From an overall view, the antenna behaves quite similarly to the typical printed monopole. The gain of the proposed antenna decreases sharply at the notched bands of 3.5/5.2 GHz, as illustrated in Figure 10. Another critical parameter for UWB antenna, the group delay, is depicted in Figure 11. As observed, small group delay variation is achieved apart from the notched bands.

4. CONCLUSION

A novel Bluetooth and UWB antenna with dual notched bands is presented and investigated. The parasitic-coupled monopole antenna exhibits UWB performance, while providing extra resonant mode and dual notched bands. The realized methodologies are by attaching additional strips along the parasitic patch, carving SRR slot on main patch and placing square patch close to feedline, respectively. Furthermore, acceptable radiation patterns, stable gain and small group delay variation are also obtained across the operation bands. Consequently, the proposed antenna could be promising for Bluetooth and UWB applications.

REFERENCES

1. First Report and Order, "Revision of Part 15 of the commission's rule regarding ultra-wideband transmission system FCC02-48," Federal Communications Commission, 2002.
2. Liang, J., C. C. Chiau, X. Chen, and C. G. Parini, "Study of a printed circular disk monopole antenna for UWB systems," *IEEE Trans. Antennas Propag.*, Vol. 33, No. 11, 3500–3504, 2005.
3. Nguyen, T. D., D. H. Lee, and H. C. Park, "Design and analysis of compact printed triple band-notched UWB antenna," *IEEE Antennas Wireless Propagat. Lett.*, Vol. 10, 403–406, 2011.
4. Liang, J., C. C. Chiau, X. Chen, and C. G. Parini, "Printed circular ring monopole antennas," *Microwave Opt. Technol. Lett.*, Vol. 45, No. 5, 372–275, 2005.
5. Beer, M., M. J. Ammann, and T. Schneider, "Electromagnetically-coupled microstrip-fed planar monopole," *Microwave Opt. Technol. Lett.*, Vol. 48, No. 1, 372–275, 2006.
6. Jung, J. H., H. Choo, and I. Park, "Design and performance of small electromagnetically coupled monopole for broadband

operation," *IET Microw. Antennas Propag.*, Vol. 1, No. 2, 536–541, 2006.

7. Chen, Z. N. and Y. W. M. Chia, "Broadband monopole antenna with parasitic planar element," *Microwave Opt. Technol. Lett.*, Vol. 27, No. 3, 209–210, 2000.
8. Eshtiaghi, R., J. Nourinia, and C. Ghobadi, "Electromagnetically coupled band-notched elliptical monopole antenna for UWB applications," *IEEE Trans. Antennas Propag.*, Vol. 58, No. 4, 1397–1402, 2010.
9. Yildirim, B. S., B. A. Cetiner, G. Roqueta, and L. Jofre, "Integrated bluetooth and UWB antenna," *IEEE Trans. Antennas Propag.*, Vol. 8, 149–152, 2009.
10. Lizzi, L., G. Oliveri, P. Rocca, and A. Massa, "Planar monopole UWB antenna with Unii1/Unii2 WLAN-band notched characteristics," *Progress In Electromagnetic Research B*, Vol. 25, 277–292, 2010.
11. Yang, Y.-B., F.-S. Zhang, L. Zhang, F. Zhang, and Y.-C. Jiao, "Design of a planar monopole antenna with dual band-notched characteristics for ultra-wideband applications," *Journal of Electromagnetic Waves and Applications*, Vol. 23, Nos. 17–18, 2481–2489, 2009.
12. Zhang, X., T.-L. Zhang, Y.-Y. Xia, Z.-H. Yan, and X.-M. Wang, "Planar monopole antenna with band-notch characterization for UWB applications," *Progress In Electromagnetics Research Letters*, Vol. 6, 149–156, 2009.
13. Kim, D.-Z., W.-I. Son, W.-G. Lim, H.-L. Lee, and J.-W. Yu, "Integrated planar monopole antenna with microstrip resonators having band-notched characteristics," *IEEE Trans. Antennas Propag.*, Vol. 58, No. 9, 2837–2842, Sep. 2010.
14. Zhang, M., Y.-Z. Yin, J. Ma, Y. Wang, W.-C. Xiao, and X.-J. Liu, "A racket-shaped slot UWB antenna coupled with parasitic strips for band-notched application," *Progress In Electromagnetic Research Letters*, Vol. 16, 35–44, 2010.
15. Peng, L. and C.-L. Ruan, "UWB band-notched monopole antenna design using electromagnetic-bandgap structure," *IEEE Trans. Microw. Theory Tech.*, Vol. 59, No. 4, 1074–1081, 2011.
16. Xie, H.-H., Y.-C. Jiao, Z. Zhang, and Y. Song, "Band-notched ultra-wideband monopole antenna using coupled resonator," *Electron. Lett.*, Vol. 46, No. 16, 2010.